# Two distinct membrane potential–dependent steps drive mitochondrial matrix protein translocation

Alexander Benjamin Schendzielorz,[1] Christian Schulz,[1] Oleksandr Lytovchenko,[1] Anne Clancy,[2] Bernard Guiard,[3] Raffaele Ieva,[4,5] Martin van der Laan,[5,6] and Peter Rehling[1,7]

[1]Department of Cellular Biochemistry and [2]Department of Molecular Biology, University Medical Center Göttingen, Georg-August-Universität Göttingen, 37073 Göttingen, Germany
[3]Centre de Génétique Moléculaire, Centre National de la Recherche Scientifique, 91190 Gif-sur-Yvette, France
[4]Laboratoire de Microbiologie et Génétique Moléculaire, Centre de Biologie Intégrative, Université de Toulouse, Centre National de la Recherche Scientifique, Unité Propre de Service, 31062 Toulouse, France
[5]Institute of Biochemistry and Molecular Biology, Center for Biochemistry and Molecular Cell Research, Faculty of Medicine, University of Freiburg, 79104 Freiburg, Germany
[6]Medical Biochemistry and Molecular Biology, Saarland University, 66421 Homburg, Germany
[7]Max Planck Institute for Biophysical Chemistry, 37077 Göttingen, Germany

Two driving forces energize precursor translocation across the inner mitochondrial membrane. Although the membrane potential ($\Delta\psi$) is considered to drive translocation of positively charged presequences through the TIM23 complex (presequence translocase), the activity of the Hsp70-powered import motor is crucial for the translocation of the mature protein portion into the matrix. In this study, we show that mitochondrial matrix proteins display surprisingly different dependencies on the $\Delta\psi$. However, a precursor's hypersensitivity to a reduction of the $\Delta\psi$ is not linked to the respective presequence, but rather to the mature portion of the polypeptide chain. The presequence translocase constituent Pam17 is specifically recruited by the receptor Tim50 to promote the transport of hypersensitive precursors into the matrix. Our analyses show that two distinct $\Delta\psi$-driven translocation steps energize precursor passage across the inner mitochondrial membrane. The $\Delta\psi$- and Pam17-dependent import step identified in this study is positioned between the two known energy-dependent steps: $\Delta\psi$-driven presequence translocation and adenosine triphosphate–driven import motor activity.

## Introduction

About two thirds of mitochondrial precursor proteins use N-terminal presequences as targeting signals (Vögtle et al., 2009). The presequence translocase (TIM23 complex) mediates transport of these precursors across the inner membrane (Neupert and Herrmann, 2007; Schulz et al., 2015). Initially, precursors are transported from the cytosol into the intermembrane space by the TOM complex in the outer membrane and are passed to the TIM23 complex (Chacinska et al., 2009; Endo and Yamano, 2010). Presequence-containing precursors can be subdivided into two classes: (1) precursors fully translocated across the inner membrane into the matrix and (2) precursors released from the translocase into the lipid phase of the inner membrane (inner membrane sorting). Precursor transport across the inner membrane is initially driven by the mitochondrial membrane potential ($\Delta\psi$) that acts on the positively charged presequences (Schleyer et al., 1982; Roise and Schatz, 1988; Martin et al., 1991; Chacinska et al., 2009; Endo and Yamano, 2010; Schulz et al., 2015; Turakhiya et al., 2016). The $\Delta\psi$ draws the presequence of the polypeptide chain through the protein-conducting channel by electrophoretic force. This energy suffices to direct laterally sorted precursors into the inner membrane (van der Laan et al., 2007). However, translocation into the matrix requires ATP hydrolysis by the presequence translocase-associated motor (PAM), in addition to the $\Delta\psi$ (Neupert and Brunner, 2002; Schulz et al., 2015).

The presequence translocase consists of a channel-forming module formed by Tim23 and Tim17. Tim50 acts as the receptor for presequences (Meinecke et al., 2006; Qian et al., 2011; Schulz et al., 2011). In addition to these essential proteins, Tim21 and Mgr2 are also constituents of the TIM23 complex. Tim21 is specific to the "motor-free" state of the translocase and enables its association with proton-pumping respiratory chain complexes (van der Laan et al., 2006). Mgr2 is positioned at the lateral gate of the translocase to regulate inner membrane sorting (Gebert et al., 2012; Ieva et al., 2014) and participates in the dynamics of the mitochondrial import motor (Schulz and Rehling, 2014). For transport of matrix proteins, the import motor is recruited to the TIM23 complex. Its central force-generating constituent is mtHsp70 (Ungermann et al., 1994; Mapa et al., 2010). Whereas Tim44 positions mtHsp70 at the channel exit for precursor engagement (Liu et al., 2003), the Pam16/18 complex regulates its ATPase activity (D'Silva et al., 2003; Truscott et al., 2003; Kozany et al., 2004). In addition, Pam17 was

Correspondence to Peter Rehling: Peter.Rehling@medizin.uni-goettingen.de

Abbreviations used: CCCP, carbonyl cyanide m-chlorophenyl hydrazone; DHFR, dihydrofolate reductase; MTX, methotrexate; PK, proteinase K; WT, wild type.



The Rockefeller University Press $30.00
J. Cell Biol. Vol. 216 No. 1 83–92
https://doi.org/10.1083/jcb.201607066

suggested as a subunit or assembly factor of the import motor (van der Laan et al., 2005; Hutu et al., 2008). However, its molecular function has remained enigmatic.

In this study, we demonstrate that mitochondrial precursors differ significantly with regard to their $\Delta\psi$ requirement for import. In contrast to the current view of how $\Delta\psi$ energizes the translocation process, we find that a precursor's hypersensitivity to the reduction of $\Delta\psi$ ($\Delta\psi$ hypersensitivity) is independent of its presequence but rather is linked to the mature portion of the polypeptide chain. Pam17 recruitment by the receptor Tim50 is specifically required for the import of these $\Delta\psi$-hypersensitive precursors but is largely dispensable for import of precursors with low $\Delta\psi$ sensitivity. Accordingly, the $\Delta\psi$ energizes a second step in matrix translocation in a presequence-independent manner.

## Results

### Matrix-destined precursor proteins display differential dependencies on Tim50

Tim50 is the major presequence receptor of the TIM23 complex in the inner mitochondrial membrane and regulates gating of the Tim23 pore. A surprising and still unresolved observation is that a loss of Tim50 leads to robust import defects for matrix proteins, but has a much lesser effect on precursors sorted into the inner membrane (Geissler et al., 2002). To assess the function of Tim50 in protein transport, we isolated mitochondria from *Saccharomyces cerevisiae* cells in which *TIM50* was under control of the *GAL1* promoter. Growing yeast in glucose-containing medium represses the *GAL1* promoter and concomitantly blocks transcription of *TIM50*. To avoid secondary effects, levels of Tim50 were maintained at 20% of the wild-type (WT) amount. Under these conditions, the protein levels of other TIM23 complex components were similar between Tim50-depleted and WT mitochondria (Fig. 1 A). Because Tim50 regulates Tim23 channel activity, we assessed $\Delta\psi$ in mitochondria with reduced amounts of Tim50 using a potential-sensitive dye. Tim50-depleted and WT mitochondria were equally able to quench the fluorescent dye, indicating that the mitochondrial $\Delta\psi$ was not affected under our conditions of controlled Tim50 depletion (Fig. 1 B). We assessed the import capacity of matrix proteins in Tim50-depleted mitochondria with in vitro transport assays. Import of $F_1\beta$ and the model matrix protein $b_2(167)_\Delta$–dihydrofolate reductase (DHFR), which consists of an N-terminal portion of cytochrome $b_2$ fused to DHFR, was strongly affected, whereas inner membrane–sorted precursors (e.g., cytochrome $c_1$) were much less Tim50 dependent, as previously reported (Fig. 1, C and D; and Fig. S1 A; Geissler et al., 2002). Considering that Tim50 serves as a presequence receptor in the intermembrane space and hence acts upstream of the import motor, the stronger reliance of motor-dependent substrates on Tim50, compared with motor-independent precursors, is surprising and still lacks an explanation (Geissler et al., 2002). To better understand the Tim50 dependence of mitochondrial proteins, we imported other matrix-targeted precursor proteins, like Tim44, a component of the import motor, and $F_1\alpha$, a soluble subunit of the $F_1F_o$-ATP synthase. Surprisingly, the import of both precursor proteins was only mildly affected in Tim50-depleted mitochondria (Fig. 1, E and F). In fact, the import efficiency was similar to the mild import defect observed for inner membrane–sorted precursor proteins (Geissler et al., 2002).

To ascertain that the observed import defects were directly linked to Tim50 function, we screened for temperature-conditional *tim50* mutants (Fig. S1 B). The mutant *tim50-19* was selected for analysis because purified mitochondria exhibited WT-like $\Delta\psi$ (Fig. S1 C). Upon heat shock of isolated mitochondria, import of $F_1\alpha$ was clearly more efficient than $F_1\beta$ in *tim50-19* mitochondria (Fig. S1, D and E). Importantly, steady-state levels of mitochondrial proteins in *tim50-19* mitochondria were similar to WT (Fig. S1 F). We conclude that impairment of Tim50 function, either by depletion of the protein or by mutagenesis of the *TIM50* gene, affects the import of different matrix proteins to different extents.

### Tim50 is important for Pam17 recruitment

To assess whether depletion of Tim50 affects TIM23 complex organization, we immunoisolated the TIM23 complex with Tim23-specific antibodies. No significant differences of the tested motor or core complex constituents associated with Tim23 were apparent. However, although steady-state levels of Pam17 were WT-like in Tim50-depleted mitochondria (Fig. 1 A), the amount of Pam17 copurified with Tim23 was drastically reduced (Fig. 2 A). A lack of Pam17 leads to a matrix protein import defect (van der Laan et al., 2005; Schiller, 2009). However, only a small set of model matrix proteins had been tested as import substrates. We therefore assessed whether import defects of *pam17Δ* mitochondria resembled those of Tim50-depleted mitochondria. To exclude unspecific effects, we confirmed that the $\Delta\psi$ was not affected in *pam17Δ* mutant mitochondria (Fig. 2 C) and in intact yeast cells (Figs. 2 B and S1 G). As reported, import of $b_2(167)_\Delta$-DHFR and $F_1\beta$ was strongly affected in *pam17Δ* mitochondria (Fig. 2, D and E; van der Laan et al., 2005). In addition, import of Pam18 and Atp14 depended on Pam17 (Fig. S2, A and C). In contrast, import of $F_1\alpha$, Tim44, Atp5, and Mdj1 was only mildly affected in the absence of Pam17 (Fig. 2, F and G; and Fig. S2, B and D). Interestingly, this differential matrix import phenotype resembled the defects observed in mitochondria with reduced Tim50 levels (Fig. 2 H). To exclude the possibility that the observed differences in *pam17Δ* mitochondria were caused by different dependencies of the precursors on import motor activity, we imported $F_1\alpha$ and $F_1\beta$ into mitochondria isolated from temperature-conditional mtHsp70 (Ssc1 in yeast) mutant cells (*ssc1-3*). For this, *ssc1-3* cells were grown at a permissive temperature, and the phenotype was induced by shifting purified mitochondria to a nonpermissive temperature before the import reaction. After heat inactivation of mtHsp70, the import of both precursors, $F_1\alpha$ and $F_1\beta$, was compromised, demonstrating that both precursors depend to the same extent on motor function (Fig. S2, E and F). To assess whether Pam17-dependent precursors also accumulated in vivo, we generated cell lysates from WT and *pam17Δ* mutant cells. As expected, we found that the precursor of Atp14 was detectable in *pam17Δ* cells. Moreover, the amount of Pam18 was drastically reduced in the *pam17Δ* mutant (Fig. S2 G).

### Pam17 affects matrix protein import independent of motor function

The selective role of Pam17 in matrix protein import suggested that Pam17 participates in import motor function (van der Laan et al., 2005). We therefore directly assessed the inward-driving force generated by the motor in WT and *pam17Δ* mitochondria. To this end, radiolabeled $b_2(167)_\Delta$-DHFR was imported into

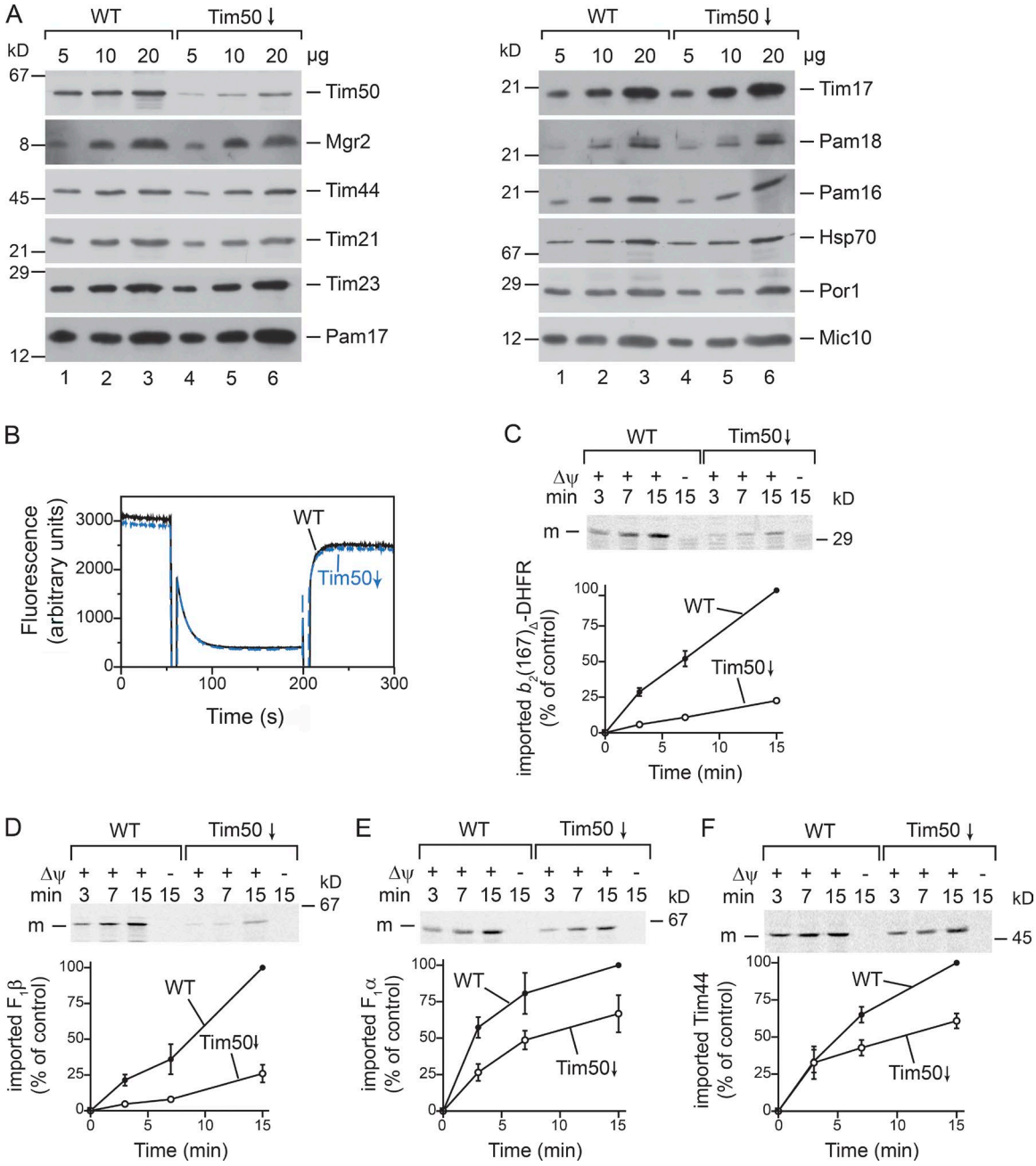


Figure 1. **Protein import is impaired in Tim50-depleted mitochondria.** (A) Steady-state Western blot analysis of WT and Tim50-depleted mitochondria. (B) Δψ of isolated mitochondria was assessed using the Δψ-sensitive dye $DiSC_3(5)$. Fluorescence was recorded before and after addition of valinomycin. (C–F) $^{35}S$-labeled precursors were imported into isolated mitochondria, and import stopped at the indicated time points with antimycin A, valinomycin, and oligomycin (AVO). Samples were PK treated and analyzed by SDS-PAGE and autoradiography. Results are presented as mean ± SEM. $n = 3$. The longest import time of the WT sample was set to 100%. m, mature protein.

mitochondria in the presence of methotrexate (MTX). MTX leads to a tight folding of the C-terminal DHFR moiety. The unfolded N-terminal part of the precursor is imported through the TOM and TIM23 complexes, whereas the DHFR moiety is pulled tightly against the TOM complex by the import motor. After initial import, the Δψ was dissipated, and proteinase K (PK) was added after different time points. In the absence of a Δψ, the import motor prevents the precursor from backsliding. Because the tightly folded DHFR moiety only becomes protease accessible if the precursor slides back, this assay enables an estimation of the pulling force of the import motor (Voisine et al., 1999). Remarkably, *pam17Δ* mitochondria did not display a pulling defect when the model protein $b_2(167)_\Delta$-DHFR was used, whereas mutant mitochondria affected in Pam16 function showed a clear pulling defect for this precursor (Fig. 3 A). Our previous work showed that *pam17Δ* mitochondria displayed a defect in this assay when inner membrane–sorted $b_2(220)$-DHFR was used (van der Laan et al., 2005). Because of the presence of a heme-binding domain, import of this precursor into mitochondria is motor dependent. Interestingly, mitochondria lacking Mgr2 also display protease sensitivity of the accumulated $b_2(220)$-DHFR, caused by an accelerated release

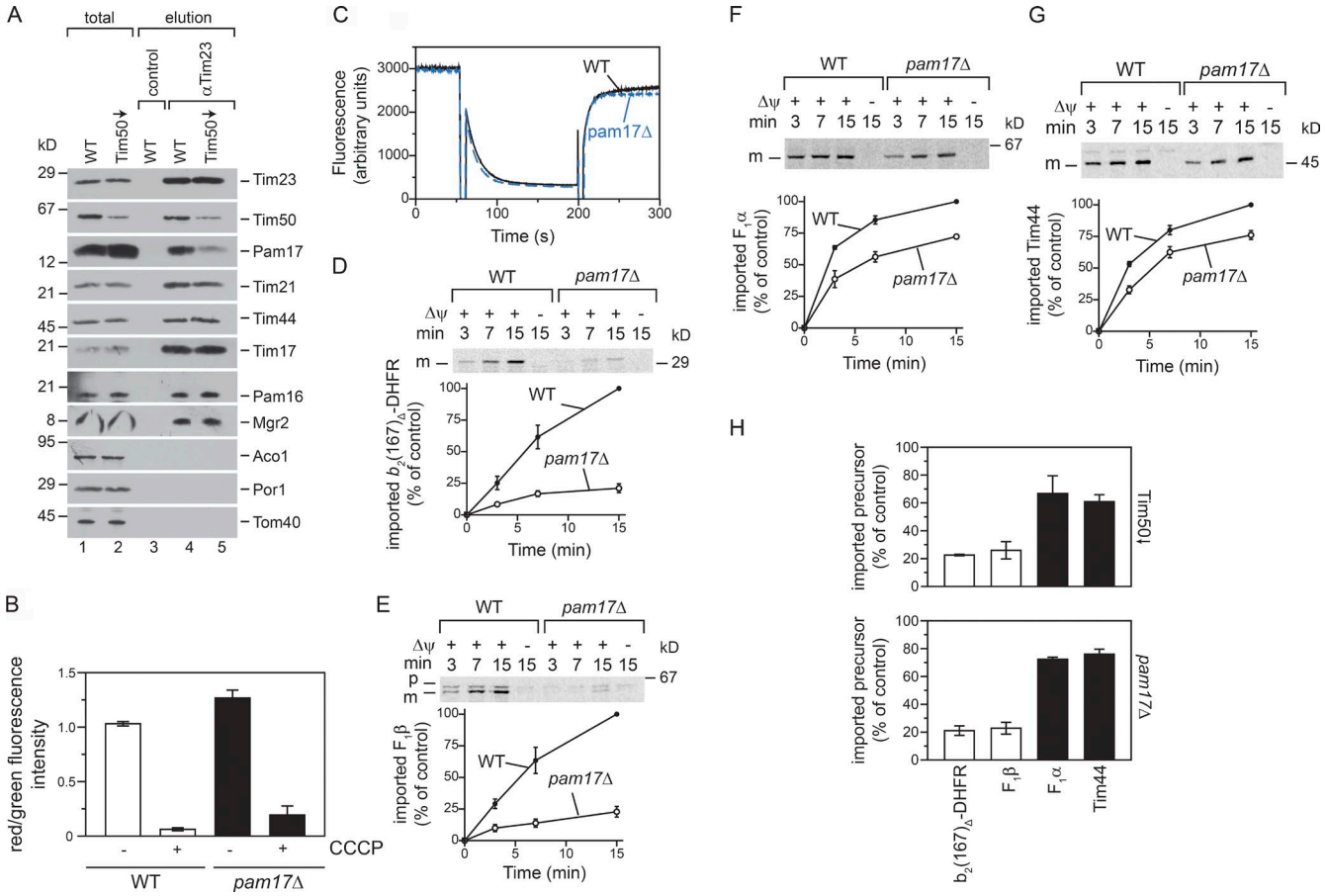


Figure 2. ***pam17Δ* mitochondria display similar import defects as mitochondria lacking Tim50.** (A) WT and Tim50-depleted mitochondria were solubilized with digitonin and subjected to α-Tim23 immunoisolation. Samples were analyzed by Western blotting. Total, 10%; elution, 100%. (B) Quantification of mean red/green fluorescence intensities from WT and *pam17Δ* cells. For each condition, three independent clones were analyzed and 150–1,500 cells were quantified. Results are presented as mean ± SEM. $n = 3$. (C) Δψ of WT and *pam17Δ* mitochondria was assessed as described in Fig. 1 B. (D–G) $^{35}$S-labeled precursors were imported as described in Fig. 1 (C–F). p, precursor; m, mature protein. (H) Comparison of import efficiency of indicated $^{35}$S-labeled precursors into Tim50-depleted or *pam17Δ* mitochondria after 15 min (results from Fig. 1 [C–F] and D–G).

from the TIM23 complex into the inner membrane (Ieva et al., 2014; Schulz and Rehling, 2014). Surprisingly, Mgr2 levels were strongly reduced in mitochondria lacking Pam17 (Fig. S3 A). Hence, we compared the ability of *mgr2Δ* mitochondria to prevent backsliding of the two precursors $b_2(167)_\Delta$-DHFR and $b_2$(220)-DHFR. A significant amount of the $b_2$(220)-DHFR intermediate became protease accessible in *mgr2Δ* mitochondria, whereas the protease sensitivity of $b_2(167)_\Delta$-DHFR was similar in WT and *mgr2Δ* mitochondria (Fig. 3 B; Ieva et al., 2014). We concluded that the apparent pulling defect in *pam17Δ* was likely an indirect defect caused by loss of Mgr2 in these mitochondria.

Pam17 dynamically associates with the TIM23 core complex, and its recruitment is triggered by presequence recognition (Popov-Celeketić et al., 2008; Lytovchenko et al., 2013). However, once a precursor spans the TOM and TIM23 complexes and engages the import motor, Pam17 is released from the translocation intermediate (Fig. S3 B). We asked whether differences between the import efficiencies of Tim44 and $F_1\alpha$, and of $F_1\beta$ and $b_2(167)_\Delta$-DHFR, were caused by distinct properties of their presequences. To test this hypothesis, the presequences of $F_1\alpha$ and $F_1\beta$ were swapped. If the presequence is the determining factor, the import defects should be reversed (Fig. 3 C). However, the presequence swap did not alter the import defects observed in mitochondria lacking either Tim50 or Pam17 (Fig. 3, D and E). Thus, the presequences do not determine the differential Tim50 and Pam17 dependence of the precursors.

## Two matrix protein classes display distinct Δψ dependencies

Because a presequence swap between $F_1\alpha$ and $F_1\beta$ did not affect their import properties in *pam17Δ* mitochondria, we investigated other factors that might be responsible for the disparities in import efficiency. Previous analyses demonstrated that the unfolding of precursors did not rescue import into *pam17Δ* mitochondria (Schiller, 2009), indicating that the folding state of the preprotein does not influence its Pam17 dependency. Therefore, we analyzed whether the tested precursors displayed characteristic differences with regard to their Δψ dependence. We imported precursors into isolated mitochondria in the absence or presence of increasing amounts of the protonophore carbonyl cyanide m-chlorophenyl hydrazone (CCCP). For all tested proteins, the import efficiency decreased with lower Δψ, as expected. However, the import of $F_1\alpha$ and Tim44 was significantly more efficient at low Δψ than the import of $F_1\beta$ and $b_2(167)_\Delta$-DHFR (Fig. 4, A–F). Compared with $F_1\alpha$ and Tim44, $F_1\beta$ and $b_2(167)_\Delta$-DHFR displayed Δψ hypersensitivity. Intriguingly, the Δψ-hypersensitive precursors were also Pam17 and

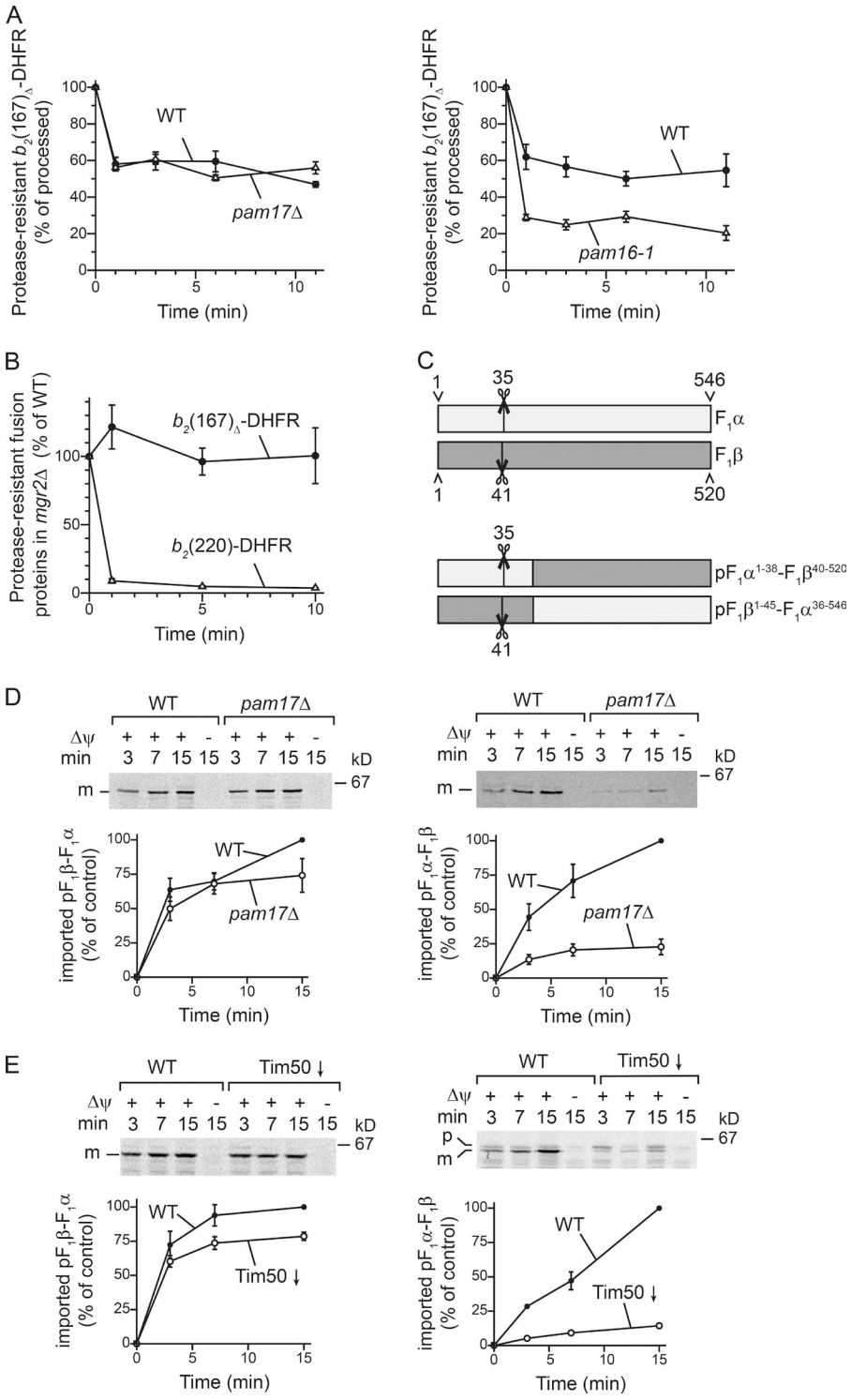


Figure 3. **Pam17 plays a motor-independent role in protein import.** (A and B) The inward driving force of the motor was assessed using $^{35}$S-labeled $b_2(167)_\Delta$-DHFR (A and B) or $b_2(220)$-DHFR (B alone) in the presence of MTX. After an initial import reaction, membrane potential was dissipated with valinomycin. The precursor was chased in a second incubation step for indicated time points before PK was added. The amount of processed intermediate was quantified (100%: amount of processed intermediate without protease treatment). Results are presented as mean ± SEM. $n$ = 3. (C) Schematic representation of $F_1\alpha$, $F_1\beta$, $pF_1\alpha$-$F_1\beta$, and $pF_1\beta$-$F_1\alpha$. For $pF_1\alpha$-$F_1\beta$, the first 38 aa of $F_1\alpha$ were fused to the mature part of $F_1\beta$ (40–end). For $pF_1\beta$-$F_1\alpha$, the first 45 aa of $F_1\beta$ were fused to the mature part of $F_1\alpha$ (36–end). (D and E) $^{35}$S-labeled $pF_1\alpha$-$F_1\beta$ and $pF_1\beta$-$F_1\alpha$ were imported into isolated mitochondria from indicated strains as described in Fig. 1. p, precursor; m, mature protein.

Tim50 dependent. This effect could also be recapitulated in vivo. When yeast cells were treated with increasing amounts of CCCP to gradually decrease the Δψ, the Pam17-dependent precursor Atp14 accumulated at a lower CCCP concentration than the Pam17-independent precursor of Mdj1 (Fig. S3 C).

The current concepts of presequence-mediated protein import into mitochondria state that the Δψ acts on positively charged residues of the presequence, and thereby drives the initial import of preproteins in an electrophoretic manner until the import motor engages with the preprotein. Accordingly, the Δψ dependence of a precursor should be mainly determined by presequence properties. However, we show that a swap of presequences between $F_1\alpha$ and $F_1\beta$ does not affect the observed import phenotype in mitochondria affected in Pam17 or Tim50 function. We therefore tested whether a presequence swap can reverse Δψ hypersensitivity of the precursor proteins. To this end, we performed CCCP titration experiments for the mature portion of $F_1\beta$ carrying the $F_1\alpha$ presequence ($pF_1\alpha$-$F_1\beta$) and the mature portion of $F_1\alpha$ fused to the presequence of $F_1\beta$ ($pF_1\beta$-$F_1\alpha$). Astonishingly, the presequence did not alter the Δψ dependence

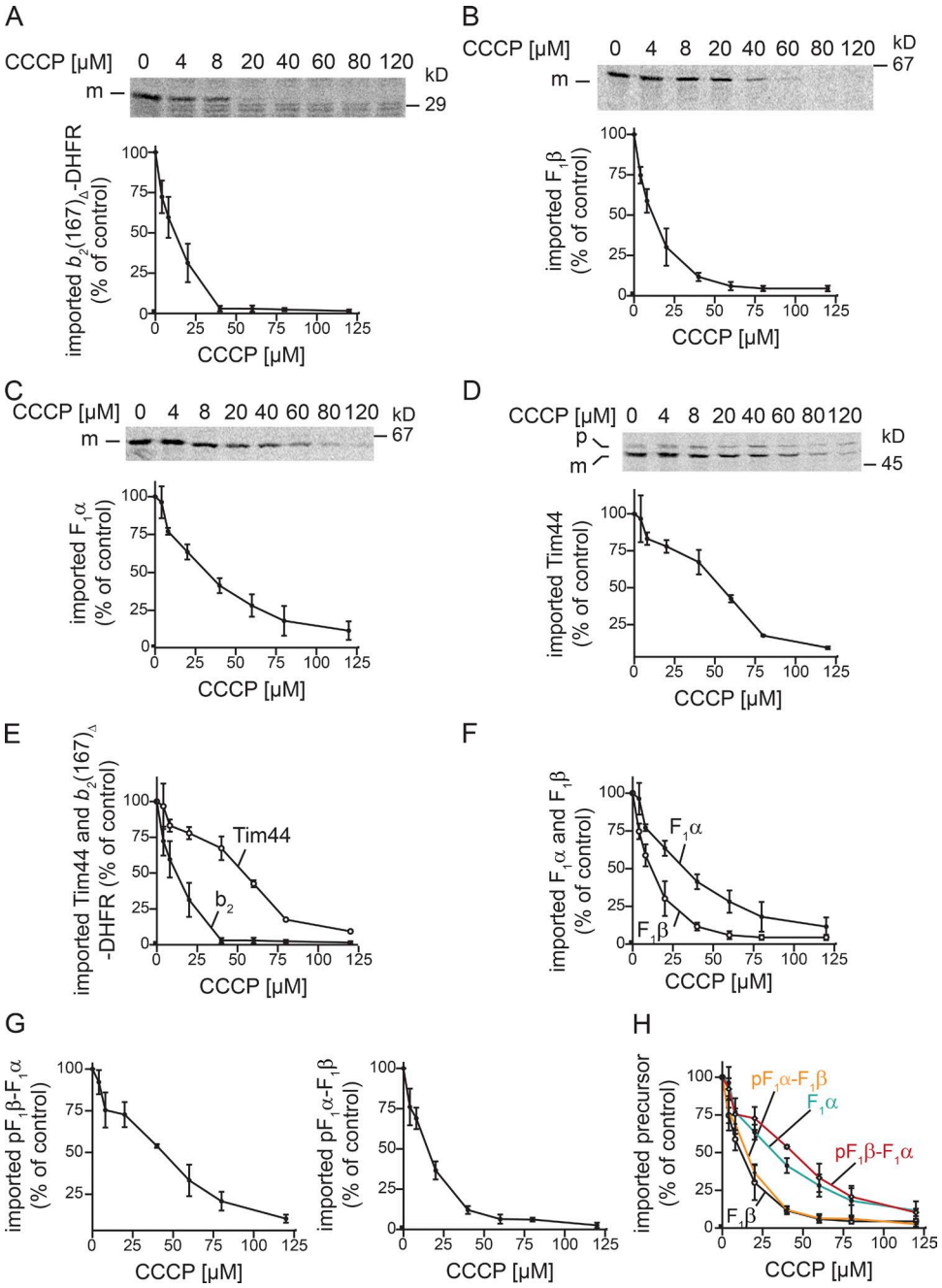


Figure 4. **Import of matrix proteins depends to different extents on membrane potential.** (A–H) Isolated WT mitochondria were treated with the indicated amounts of CCCP for 5 min before import. After 15 min of import, reactions were stopped with AVO, and import was analyzed by SDS-PAGE and digital autoradiography. Results are presented as mean ± SEM. $n = 3$. p, precursor; m, mature protein. (E and F) Overlay of results from CCCP titration experiments with $F_1\alpha$, $F_1\beta$, Tim44, and $b_2(167)_\Delta$-DHFR. (H) Overlay of results from CCCP titration experiments with $F_1\alpha$, $F_1\beta$, $pF_1\alpha$-$F_1\beta$, and $pF_1\beta$-$F_1\alpha$.

of the imported precursor, but rather the mature portion of the polypeptide determined Δψ hypersensitivity (Fig. 4, G and H). To address whether a depletion of the Δψ affects the association of Pam17 with the translocase, we immunoisolated the TIM23 complex in the presence of CCCP. At a concentration of 40 µM, when import of Δψ hypersensitivity precursors is significantly affected, Pam17 remained bound to TIM23 (Fig. S3 D). We also analyzed the association of Pam17 with Tim23 by chemical cross-linking in the presence or absence of Δψ (Hutu et al., 2008). The reported Pam17–Tim23 cross-link was not affected by CCCP addition (Fig. S3 E). Accordingly, the observed Δψ hypersensitivity of precursors is not linked to a dissociation of Pam17 from the import machinery. We conclude that in addition to the universal Δψ-driven translocation of the presequence, a second Δψ-dependent translocation step promotes the transport of the mature portion in a class of mitochondrial matrix proteins.

## Discussion

The mitochondrial Δψ is a crucial driving force for inner membrane translocation that acts on precursor proteins in the vicinity

of the inner membrane. We report that mitochondrial matrix proteins do not display a uniform dependency on Δψ. Although import of some matrix-targeted proteins is already severely impaired when the Δψ is slightly reduced, other precursors are hardly affected until Δψ is strongly compromised. Previous work defined the concept of two energy-dependent translocation stages (Chacinska et al., 2009; Neupert, 2015; Schulz et al., 2015). First, the Δψ acts on the positive charges of the presequence to drive precursor translocation in an electrophoretic manner. Second, mtHsp70 engages with precursors to energize the ATP-dependent unfolding of precursor proteins and their matrix translocation. We now show that the observed Δψ hypersensitivity of the precursors cannot be alleviated by replacement of the presequence with that of a less Δψ-dependent precursor protein. Our findings reveal an unexpected shortcoming in the current concepts of mitochondrial protein import. They confine a critical Δψ dependency also to the mature portion of matrix-targeted proteins. Accordingly, precursor translocation is facilitated by two independent Δψ-driven steps.

We show that Pam17 specifically promotes the transport of Δψ-hypersensitive precursors into the matrix and that the presequence receptor Tim50 is critical for efficient Pam17 recruitment to the TIM23 channel. Consequently, mitochondria affected in Tim50 function mimic the *pam17Δ* phenotype with regard to import defects for Δψ-hypersensitive precursors. Because the Pam17 dependency of precursor proteins is determined by their mature domain and because Tim50 likely contains more than one precursor protein binding site (Qian et al., 2011; Schulz et al., 2011; Lytovchenko et al., 2013; Rahman et al., 2014), it is tempting to speculate that Tim50 may not only interact with presequences, but also with segments of the mature region of precursors. Because there are no specific mutations defined that affect Tim50's interaction with a presequence, the question of whether this domain also acts on the mature part can currently not be assessed experimentally. Our findings suggest that Tim50 may translate information about the nature of the precursor protein into an energy supply requirement. Pam17 has been considered to affect the functionality of the import motor (van der Laan et al., 2005; Hutu et al., 2008; Schiller, 2009). This model is based on matrix protein import defects observed in *pam17Δ* mutant mitochondria and the protease sensitivity of arrested $b_2$(220)-DHFR (van der Laan et al., 2005). However, in this study, we show that the matrix protein import defect in *pam17Δ* is specific for Δψ-hypersensitive precursors and that the observed protease sensitivity of $b_2$(220)-DHFR is likely caused by a loss of Mgr2, leading to enhanced lateral release of this precursor into the inner membrane. We therefore conclude that motor function is not rate limiting to the import of matrix proteins in *pam17Δ* mitochondria, but that the matrix protein import defect is linked to a Δψ-sensitive translocation step particularly affecting those precursors that are Δψ hypersensitive.

How does the Δψ affect the transport of Δψ-hypersensitive precursor proteins? Work by Huang et al. (2002) demonstrated that the Δψ participates in the unfolding of the mature portion of precursor proteins. However, this Δψ-mediated unfolding activity has been shown to depend on the precursor's presequence. In line with this, chemical unfolding of the precursor does not alleviate the *pam17Δ* import defect (Schiller, 2009). Accordingly, the Pam17 dependence and Δψ hypersensitivity of precursors does not reflect an increased unfolding requirement during import. Regarding the order of transport events at the presequence translocase, the second Δψ-dependent transport step succeeds a presequence-dependent translocation event, but precedes the motor-requiring transport stages. Pam17 was shown to directly interact with the central core component, Tim23 (Hutu et al., 2008; Popov-Celeketić et al., 2008). Of note, Δψ affects the conformation of the Tim23 protein independently of presequence binding (Malhotra et al., 2013). In this light, we propose that the Tim23 channel gating activity contributes significantly to the passage of Δψ-hypersensitive precursors. This interpretation could link the transport reaction to an unresolved behavior of the Tim23 channel. Although the Tim23 channel is activated by presequences at low Δψ, in the absence of presequences the channel displays a biphasic activity pattern. At low Δψ, the gating activity of the Tim23 channel is low; however, it becomes activated at high Δψ (Truscott et al., 2001; van der Laan et al., 2007). Our analyses are in agreement with the idea that Δψ-hypersensitive precursors especially depend on this second, presequence-independent channel activation step, which may be facilitated by Pam17 recruitment to the import channel.

## Materials and methods

### Yeast growth and handling

Yeast strains were grown in YP medium (1% yeast extract and 2% peptone) containing 2% glucose (YPD) or 3% glycerol (YPG) at 30°C. *pam17Δ* (van der Laan et al., 2005), *pam16-1* (Frazier et al., 2004), and corresponding WT strains were grown at 25°C, except for the experiment described in Fig. S2 G, for which *pam17Δ* and WT cells were grown at 30°C. *mgr2Δ* and the corresponding WT strain were shifted to 39°C for 24 h before harvesting (Gebert et al., 2012). A strain in which the *TIM50* gene was under the control of a *GAL1* promoter was described previously (Geissler et al., 2002). For down-regulation of Tim50 expression, yeast cells were precultured in YP medium containing 2% galactose, 1% raffinose, and 3% lactate, pH 5.0, and subsequently grown for 38 h at 30°C in YP medium containing 3% lactate, pH 5.0, and 0.2% glucose. In the absence of galactose and presence of glucose, the *GAL1* promoter is repressed. Consequently, Tim50 levels are reduced as a result of protein turnover and cell division.

For the generation of the temperature-sensitive allele *tim50-19*, a plasmid-encoded WT *TIM50* allele was replaced in the corresponding gene deletion strain derived from *S. cerevisiae* YPH499 by gap repair and shuffling of a *TIM50* version obtained by error-prone PCR. Temperature-conditional alleles were selected by comparing the growth of strains at permissive and nonpermissive temperatures. Sequence analysis of the *tim50-19* allele revealed four mutations, K93N in the matrix domain, F345L and W376R in the core domain, and I422V in the C-terminal presequence-binding domain.

For detection of import defects in cells, WT and *pam17Δ* strains were grown in YPD medium at 30°C overnight. The next morning, cells were diluted to $OD_{600}$ = 0.2 and grown for 10 h in YPG at 30°C. Afterward, cells were harvested and cell lysates were analyzed by SDS-PAGE and Western blotting.

### Microscopy

To assess mitochondrial membrane potential in cells, yeast strains were grown in YPG medium supplemented with 20 mg/L adenine at 25°C overnight. The next morning, cells were harvested at $OD_{600}$ = 2–3, pelleted, and washed with 10 mM Tris/HCl, pH 6.8. Next, cells were incubated with 20 µM CCCP or the same volume of ethanol for 5 min at 25°C before addition of 2 µM JC-1. After 10 min of incubation at

25°C, cells were washed three times with 10 mM Tris/HCl, pH 6.8, and analyzed by microscopy.

For this, a 1:25 dilution of cells in a 384-well microtitre plate was automatically imaged at 30°C on an Imaging Machine 03-dual widefield high content screening microscope (Acquifer) equipped with a white light-emitting diode array for brightfield imaging, a light-emitting diode fluorescence excitation light source, an sCMOS (2,048 × 2,048 pixel) camera, a temperature-controlled incubation chamber, and a stationary plate holder in combination with movable optics. Images were acquired in brightfield and with 470-nm and 590-nm filter cubes (exitation 469/35 nm, emission 525/39 nm, and dichroic 497 nm; and exitation 590/20 nm, emission 628/32 nm, and dichroic 607 nm; respectively) with a 40× CFI Super Plan Fluor ELWD NA 0.60 (Nikon). Integration times were fixed at 200 ms for both fluorescence channels. The focal plane was detected in the brightfield channel using a yeast autofocus algorithm.

Fluorescence was quantified using a Knime (Berthold et al., 2009) pipeline to automate segmentation of the individual cells in the brightfield channel, followed by quantification of the mean cell fluorescence in both channels.

### Import of precursor proteins

Precursor proteins were radiolabeled by translation in the presence of [$^{35}$S]methionine using rabbit reticulocyte lysate (Promega). Mitochondria were resuspended in import buffer (250 mM sucrose, 10 mM MOPS/KOH, pH 7.2, 80 mM KCl, 2 mM $KH_2PO_4$, 5 mM $MgCl_2$, 5 mM methionine, and 3% fatty acid–free BSA) supplemented with 2 mM ATP and 2 mM NADH. Membrane potential was dissipated using a final concentration of 8 µM antimycin A, 1 µM valinomycin, and 20 µM oligomycin. 20-µg/ml PK treatment was performed for 10 min on ice. 2 mM PMSF was added for 10 min on ice to inactivate PK. Mitochondria were sedimented, washed with SEM (250 mM sucrose, 1 mM EDTA, and 20 mM MOPS, pH 7.2) and further analyzed by SDS-PAGE and autoradiography. Quantifications were performed using ImageQuant TL (GE Healthcare) using a rolling ball background subtraction.

### Protein complex isolation

Coimmunoprecipitation experiments using Tim23-specific serum were performed essentially as described previously (Herrmann et al., 2001). In brief, mitochondria were resuspended to 1 mg/ml in solubilization buffer (20 mM Tris/HCl, pH 7.4, 150 mM NaCl, 10% glycerol [wt/vol], 1 mM PMSF, and 1% digitonin) and incubated for 30 min on ice. After a clarifying spin, supernatant was loaded on protein A–Sepharose beads cross-linked to Tim23 antibodies, incubated for 1.5 h at 4°C on a rotating wheel, washed 10× (solubilization buffer with 0.3% digitonin), and eluted with a 50-µl double-bed volume of 0.1 M glycine, pH 2.8 (neutralized with 1-M Tris base). To address Pam17 association with the TIM23 complex at low membrane potential, mitochondria were incubated with CCCP in solubilization buffer lacking digitonin for 5 min on ice before solubilization with 1% (wt/vol) digitonin and coimmunoprecipitation.

### Membrane potential measurements

Mitochondrial membrane potential was assessed using 3,3′-dipropylthiadicarbocyanine iodide ($DiSC_3(5)$). Mitochondria were suspended in buffer containing 600 mM sorbitol, 1% (wt/vol) BSA, 10 mM $MgCl_2$, and 20 mM KPi, pH 7.4, to a concentration of 166 µg/ml. Changes in fluorescence were recorded using a F-7000 fluorescence spectrophotometer (Hitachi) at 25°C with excitation at 622 nm, emission at 670 nm, and slits of 5 nm. Components were added to the cuvette containing 500 µl of buffer in the following order: $DiSC_3(5)$, 83 µg of mitochondria, and valinomycin (5 µl from 100-µM stock in EtOH, 1 µM final) to dissipate the membrane potential. The difference in fluorescence before and after the addition of valinomycin was used to compare relative membrane potential between strains.

### Cloning

Presequence swap of *Neurospora crassa* $F_1\beta$ and *S. cerevisiae* $F_1\alpha$ was performed by overlap PCR. For $pF_1\alpha$-$F_1\beta$, the first 38 aa of yeast $F_1\alpha$ were fused to the mature part of *N. crassa* $F_1\beta$ (40–end). For $pF_1\beta$-$F_1\alpha$, the first 45 aa of $F_1\beta$ were fused to the mature part of $F_1\alpha$ (36–end).

### Assessing import-driving activity

Import-driving activity was assessed as previously described (Voisine et al., 1999). For import experiments, temperature-sensitive strains were incubated in import buffer for 15 min at 37°C, and subsequently 2 mM ATP, 2 mM NADH, 5 mM creatine phosphate, and 0.01 mg/ml creatine kinase were added. Radiolabeled $b_2(167)_\Delta$-DHFR was imported at 25°C for 15 min in the presence of 5 µM MTX, and membrane potential was dissipated using 1 µM valinomycin. A sample was taken ($\Delta t = 0$ min), the precursor was chased at 25°C, and samples were treated with PK after 1, 3, 6, and 11 min for 15 min on ice. Samples were analyzed by SDS-PAGE and autoradiography. The amount of PK-resistant intermediate was quantified and standardized to the total amount of generated intermediate ($\Delta t = 0$) for each strain.

### Membrane potential reduction by CCCP titration

For reduction of membrane potential, the protonophore CCCP was used as previously reported (van der Laan et al., 2006). Mitochondria were resuspended in import buffer with 1% BSA and 20 µM oligomycin to prevent regeneration of membrane potential by the reverse function of the $F_1F_o$-ATPase. CCCP was added from a 4 mM stock in EtOH, and mitochondria were incubated for 5 min at 25°C before import.

For in vivo CCCP titration, cells were grown at 30°C overnight in YPD medium. The next day, cells were diluted to $OD_{600} = 0.5$ in 2× YPAD, and grown for another 5 h. Then, cells were diluted back to $OD_{600} = 1$ in 2× YPAD, and CCCP was added from a 50 mM stock solution. After 30 min of incubation, cells were harvested and cell lysates were analyzed by SDS-PAGE and Western blotting. For quantification, the amount of accumulated precursor at 80 µM CCCP was set to 100%.

### Chemical cross-linking

For cross-linking, mitochondria were resuspended in import buffer without BSA to a final concentration of 1 mg/ml. CCCP was added from a 5 mM stock solution, and mitochondria were incubated for 5 min on ice. Next, disuccinimidyl glutarate in DMSO was added to a final concentration of 500 µM, and mitochondria were incubated for 30 min on ice. Afterward, excess cross-linker was quenched using 100 mM glycine, pH 8.0, for 10 min on ice. After reisolation of mitochondria, cross-links were analyzed by SDS-PAGE and Western blotting.

### Generation and isolation of the TIM23–TOM supercomplex

A TIM23–TOM supercomplex was isolated essentially as described previously (Chacinska et al., 2003). In brief, recombinant $b_2(167)_\Delta$-DHFR was imported into mitochondria in import buffer with BSA in the presence of 5 µM MTX for 15 min at 25°C. Next, mitochondria were reisolated, washed with SEM, resuspended to 1 mg/ml in solubilization buffer (20 mM Tris/HCl, pH 7.4, 150 mM NaCl, 10% glycerol [wt/vol], 1 mM PMSF, and 1% digitonin), and incubated for 30 min on ice. After a clarifying spin, complexes were isolated by incubating lysates with Tim23- or Tom22-specific antibodies coupled to protein A–Sepharose beads. Beads were washed 10× with solubilization buffer containing 0.3% (wt/vol) digitonin and eluted with 100 mM glycine, pH 2.8.

### Isolation of mitochondria

Mitochondria were isolated essentially as previously described (Meisinger et al., 2006). If not stated otherwise, yeast cells were grown in YPG medium and harvested at $OD_{600}$ = 2–3. After treatment with buffer A (10 mM DTT and 100 mM Tris/$H_2SO_4$, pH 9.4) for 30 min at 30°C, cells were washed and treated with zymolyase buffer (20 mM $KPO_4$, pH 7.4, 1.2 M sorbitol, and 0.57 mg/L zymolyase) for 1–2 h at 30°C. After additional washing in zymolyase buffer without enzyme, cells were resuspended in ice-cold homogenization buffer (600 mM sorbitol, 10 mM Tris/HCl, pH 7.4, 1 g/L BSA, 1 mM PMSF, and 1 mM EDTA) and opened using a cell homogenizer. The mitochondrial fraction was obtained by differential centrifugation, resuspended in SEM buffer, and frozen in liquid nitrogen.

### Online supplemental material

Fig. S1 shows corresponding import experiments to Fig. 1 in *tim50-19* mitochondria. Moreover, in vivo membrane potential assessment in *pam17Δ* cells and WT cells are shown. Fig. S2 shows precursor imports in *pam17Δ* mitochondria and in vivo precursor accumulation, extending Fig. 2 (D–G). Also, $F_1\alpha$ and $F_1\beta$ imports in *ssc1-3* mitochondria show that both precursors are to the same extent motor dependent for import. Fig. S3 relates to Fig. 3 and shows steady-state protein analysis of *pam17Δ* mitochondria and the Pam17 association with the TIM23 complex when a precursor spans both TOM and TIM23 complexes. Fig. S3 also shows in vivo CCCP titration and Pam17 association with the TIM23 complex under low-membrane potential conditions supporting data in Fig. 4.


## Acknowledgments

We thank M. Meinecke for discussion, S. Callegari for critical reading, and Á. Farkas for support in data analyses.

This work was supported by the Deutsche Forschungsgemeinschaft (DFG) grants SFB860 to P. Rehling, SFB746 to M. van der Laan, and SFB1190/Z03 to A. Clancy. This work was also supported by the Molecular Biology PhD program at the International Max Planck Research School and Göttingen Graduate School for Neurosciences and Molecular Biosciences DFG grant GSC 226/1 to A.B. Schendzielorz and C. Schulz, the Excellence Initiative of the German federal and state governments EXC 294 BIOSS grant to M. van der Laan, the Centre National de la Recherche Scientifique–Institut National de la Santé et de la Recherche Médicale ATIP-Avenir program grant to R. Ieva, Boehringer Ingelheim Fonds grant to C. Schulz, and the Max Planck Society (to P. Rehling).

The authors declare no competing financial interests.

Submitted: 18 July 2016
Revised: 30 September 2016
Accepted: 28 November 2016


## References


Berthold, M.R., N. Cebron, F. Dill, T.R. Gabriel, T. Kötter, T. Meinl, P. Ohl, K. Thiel, and B. Wiswedel. 2009. KNIME - the konstanz information miner: version 2.0 and beyond. *SIGKDD Explor.* 11:26–31. http://dx.doi.org/10.1145/1656274.1656280

Chacinska, A., P. Rehling, B. Guiard, A.E. Frazier, A. Schulze-Specking, N. Pfanner, W. Voos, and C. Meisinger. 2003. Mitochondrial translocation contact sites: separation of dynamic and stabilizing elements in formation of a TOM-TIM-preprotein supercomplex. *EMBO J.* 22:5370–5381. http://dx.doi.org/10.1093/emboj/cdg532

Chacinska, A., C.M. Koehler, D. Milenkovic, T. Lithgow, and N. Pfanner. 2009. Importing mitochondrial proteins: machineries and mechanisms. *Cell.* 138:628–644. http://dx.doi.org/10.1016/j.cell.2009.08.005

D'Silva, P.D., B. Schilke, W. Walter, A. Andrew, and E.A. Craig. 2003. J protein cochaperone of the mitochondrial inner membrane required for protein import into the mitochondrial matrix. *Proc. Natl. Acad. Sci. USA.* 100:13839–13844. http://dx.doi.org/10.1073/pnas.1936150100

Endo, T., and K. Yamano. 2010. Transport of proteins across or into the mitochondrial outer membrane. *Biochim. Biophys. Acta.* 1803:706–714. http://dx.doi.org/10.1016/j.bbamcr.2009.11.007

Frazier, A.E., J. Dudek, B. Guiard, W. Voos, Y. Li, M. Lind, C. Meisinger, A. Geissler, A. Sickmann, H.E. Meyer, et al. 2004. Pam16 has an essential role in the mitochondrial protein import motor. *Nat. Struct. Mol. Biol.* 11:226–233. http://dx.doi.org/10.1038/nsmb735

Gebert, M., S.G. Schrempp, C.S. Mehnert, A.K. Heißwolf, S. Oeljeklaus, R. Ieva, M. Bohnert, K. von der Malsburg, S. Wiese, T. Kleinschroth, et al. 2012. Mgr2 promotes coupling of the mitochondrial presequence translocase to partner complexes. *J. Cell Biol.* 197:595–604. http://dx.doi.org/10.1083/jcb.201110047

Geissler, A., A. Chacinska, K.N. Truscott, N. Wiedemann, K. Brandner, A. Sickmann, H.E. Meyer, C. Meisinger, N. Pfanner, and P. Rehling. 2002. The mitochondrial presequence translocase: an essential role of Tim50 in directing preproteins to the import channel. *Cell.* 111:507–518. http://dx.doi.org/10.1016/S0092-8674(02)01073-5

Herrmann, J.M., B. Westermann, and W. Neupert. 2001. Analysis of protein–protein interactions in mitochondria by coimmunoprecipitation and chemical cross-linking. *Methods Cell Biol.* 65:217–230. http://dx.doi.org/10.1016/S0091-679X(01)65013-1

Huang, S., K.S. Ratliff, and A. Matouschek. 2002. Protein unfolding by the mitochondrial membrane potential. *Nat. Struct. Biol.* 9:301–307. http://dx.doi.org/10.1038/nsb772

Hutu, D.P., B. Guiard, A. Chacinska, D. Becker, N. Pfanner, P. Rehling, and M. van der Laan. 2008. Mitochondrial protein import motor: differential role of Tim44 in the recruitment of Pam17 and J-complex to the presequence translocase. *Mol. Biol. Cell.* 19:2642–2649. http://dx.doi.org/10.1091/mbc.E07-12-1226

Ieva, R., S.G. Schrempp, L. Opaliński, F. Wollweber, P. Höß, A.K. Heißwolf, M. Gebert, Y. Zhang, B. Guiard, S. Rospert, et al. 2014. Mgr2 functions as lateral gatekeeper for preprotein sorting in the mitochondrial inner membrane. *Mol. Cell.* 56:641–652. http://dx.doi.org/10.1016/j.molcel.2014.10.010

Kozany, C., D. Mokranjac, M. Sichting, W. Neupert, and K. Hell. 2004. The J domain–related cochaperone Tim16 is a constituent of the mitochondrial TIM23 preprotein translocase. *Nat. Struct. Mol. Biol.* 11:234–241. http://dx.doi.org/10.1038/nsmb734

Liu, Q., P. D'Silva, W. Walter, J. Marszalek, and E.A. Craig. 2003. Regulated cycling of mitochondrial Hsp70 at the protein import channel. *Science.* 300:139–141. http://dx.doi.org/10.1126/science.1083379

Lytovchenko, O., J. Melin, C. Schulz, M. Kilisch, D.P. Hutu, and P. Rehling. 2013. Signal recognition initiates reorganization of the presequence translocase during protein import. *EMBO J.* 32:886–898. http://dx.doi.org/10.1038/emboj.2013.23

Malhotra, K., M. Sathappa, J.S. Landin, A.E. Johnson, and N.N. Alder. 2013. Structural changes in the mitochondrial Tim23 channel are coupled to the proton-motive force. *Nat. Struct. Mol. Biol.* 20:965–972. http://dx.doi.org/10.1038/nsmb.2613

Mapa, K., M. Sikor, V. Kudryavtsev, K. Waegemann, S. Kalinin, C.A.M. Seidel, W. Neupert, D.C. Lamb, and D. Mokranjac. 2010. The conformational dynamics of the mitochondrial Hsp70 chaperone. *Mol. Cell.* 38:89–100. http://dx.doi.org/10.1016/j.molcel.2010.03.010

Martin, J., K. Mahlke, and N. Pfanner. 1991. Role of an energized inner membrane in mitochondrial protein import. Delta psi drives the movement of presequences. *J. Biol. Chem.* 266:18051–18057.

Meinecke, M., R. Wagner, P. Kovermann, B. Guiard, D.U. Mick, D.P. Hutu, W. Voos, K.N. Truscott, A. Chacinska, N. Pfanner, and P. Rehling. 2006. Tim50 maintains the permeability barrier of the mitochondrial inner membrane. *Science.* 312:1523–1526. http://dx.doi.org/10.1126/science.1127628

Meisinger, C., N. Pfanner, and K.N. Truscott. 2006. Isolation of yeast mitochondria. *Methods Mol. Biol.* 313:33–39.

Neupert, W. 2015. A perspective on transport of proteins into mitochondria: a myriad of open questions. *J. Mol. Biol.* 427:1135–1158. http://dx.doi.org/10.1016/j.jmb.2015.02.001

Neupert, W., and M. Brunner. 2002. The protein import motor of mitochondria. *Nat. Rev. Mol. Cell Biol.* 3:555–565. http://dx.doi.org/10.1038/nrm878

Neupert, W., and J.M. Herrmann. 2007. Translocation of proteins into mitochondria. *Annu. Rev. Biochem.* 76:723–749. http://dx.doi.org/10.1146/annurev.biochem.76.052705.163409

Popov-Celeketić, D., K. Mapa, W. Neupert, and D. Mokranjac. 2008. Active remodelling of the TIM23 complex during translocation of preproteins into mitochondria. *EMBO J.* 27:1469–1480.

Qian, X., M. Gebert, J. Höpker, M. Yan, J. Li, N. Wiedemann, M. van der Laan, N. Pfanner, and B. Sha. 2011. Structural basis for the function of Tim50 in the mitochondrial presequence translocase. *J. Mol. Biol.* 411:513–519. http://dx.doi.org/10.1016/j.jmb.2011.06.020

Rahman, B., S. Kawano, K. Yunoki-Esaki, T. Anzai, and T. Endo. 2014. NMR analyses on the interactions of the yeast Tim50 C-terminal region with the presequence and Tim50 core domain. *FEBS Lett.* 588:678–684. http://dx.doi.org/10.1016/j.febslet.2013.12.037

Roise, D., and G. Schatz. 1988. Mitochondrial presequences. *J. Biol. Chem.* 263:4509–4511.

Schiller, D. 2009. Pam17 and Tim44 act sequentially in protein import into the mitochondrial matrix. *Int. J. Biochem. Cell Biol.* 41:2343–2349. http://dx.doi.org/10.1016/j.biocel.2009.06.011

Schleyer, M., B. Schmidt, and W. Neupert. 1982. Requirement of a membrane potential for the posttranslational transfer of proteins into mitochondria. *Eur. J. Biochem.* 125:109–116. http://dx.doi.org/10.1111/j.1432-1033.1982.tb06657.x

Schulz, C., and P. Rehling. 2014. Remodelling of the active presequence translocase drives motor-dependent mitochondrial protein translocation. *Nat. Commun.* 5. http://dx.doi.org/10.1038/ncomms5349

Schulz, C., O. Lytovchenko, J. Melin, A. Chacinska, B. Guiard, P. Neumann, R. Ficner, O. Jahn, B. Schmidt, and P. Rehling. 2011. Tim50's presequence receptor domain is essential for signal driven transport across the TIM23 complex. *J. Cell Biol.* 195:643–656. http://dx.doi.org/10.1083/jcb.201105098

Schulz, C., A. Schendzielorz, and P. Rehling. 2015. Unlocking the presequence import pathway. *Trends Cell Biol.* 25:265–275. http://dx.doi.org/10.1016/j.tcb.2014.12.001

Truscott, K.N., P. Kovermann, A. Geissler, A. Merlin, M. Meijer, A.J. Driessen, J. Rassow, N. Pfanner, and R. Wagner. 2001. A presequence- and voltage-sensitive channel of the mitochondrial preprotein translocase formed by Tim23. *Nat. Struct. Biol.* 8:1074–1082. http://dx.doi.org/10.1038/nsb726

Truscott, K.N., W. Voos, A.E. Frazier, M. Lind, Y. Li, A. Geissler, J. Dudek, H. Müller, A. Sickmann, H.E. Meyer, et al. 2003. A J-protein is an essential subunit of the presequence translocase-associated protein import motor of mitochondria. *J. Cell Biol.* 163:707–713. http://dx.doi.org/10.1083/jcb.200308004

Turakhiya, U., K. von der Malsburg, V.A.M. Gold, B. Guiard, A. Chacinska, M. van der Laan, and R. Ieva. 2016. Protein import by the mitochondrial presequence translocase in the absence of a membrane potential. *J. Mol. Biol.* 428:1041–1052. http://dx.doi.org/10.1016/j.jmb.2016.01.020

Ungermann, C., W. Neupert, and D.M. Cyr. 1994. The role of Hsp70 in conferring unidirectionality on protein translocation into mitochondria. *Science.* 266:1250–1253. http://dx.doi.org/10.1126/science.7973708

van der Laan, M., A. Chacinska, M. Lind, I. Perschil, A. Sickmann, H.E. Meyer, B. Guiard, C. Meisinger, N. Pfanner, and P. Rehling. 2005. Pam17 is required for architecture and translocation activity of the mitochondrial protein import motor. *Mol. Cell. Biol.* 25:7449–7458. http://dx.doi.org/10.1128/MCB.25.17.7449-7458.2005

van der Laan, M., N. Wiedemann, D.U. Mick, B. Guiard, P. Rehling, and N. Pfanner. 2006. A role for Tim21 in membrane-potential-dependent preprotein sorting in mitochondria. *Curr. Biol.* 16:2271–2276. http://dx.doi.org/10.1016/j.cub.2006.10.025

van der Laan, M., M. Meinecke, J. Dudek, D.P. Hutu, M. Lind, I. Perschil, B. Guiard, R. Wagner, N. Pfanner, and P. Rehling. 2007. Motor-free mitochondrial presequence translocase drives membrane integration of preproteins. *Nat. Cell Biol.* 9:1152–1159. http://dx.doi.org/10.1038/ncb1635

Vögtle, F.-N., S. Wortelkamp, R.P. Zahedi, D. Becker, C. Leidhold, K. Gevaert, J. Kellermann, W. Voos, A. Sickmann, N. Pfanner, and C. Meisinger. 2009. Global analysis of the mitochondrial N-proteome identifies a processing peptidase critical for protein stability. *Cell.* 139:428–439. http://dx.doi.org/10.1016/j.cell.2009.07.045

Voisine, C., E.A. Craig, N. Zufall, O. von Ahsen, N. Pfanner, and W. Voos. 1999. The protein import motor of mitochondria: unfolding and trapping of preproteins are distinct and separable functions of matrix Hsp70. *Cell.* 97:565–574. http://dx.doi.org/10.1016/S0092-8674(00)80768-0